

THE VARIATION OF THE UNIVERSAL GRAVITATIONAL CONSTANT AND THE DISTRIBUTION OF EARTHQUAKES IN CHINA THROUGH TIME AND SPACE

Bruce Denness

(Bureau of Applied Sciences Wydcombe Manor, Whitwell, I. W., P038 2NY, England)

SUMMARY

Earthquakes are devastating natural disasters: no place on Earth experiences them to a greater extent than China and the East Asian seaboard. Similarly drought, floods and other climatic hazards are frequent events around the World. A theory is developed here to link these two geophysical phenomena.

During the early 1980's a deterministic analytical model of climate variation was developed. It matches proxy palaeoclimatic time series and can also be used for forecasting; it has been successfully tested for several years. Earlier substantiation of the model over geological timescales is here extended through recent history. An explanation of the cause of climate change is then suggested based on the possibility that the Universal Gravitational Constant (G) may vary with time. Variation of G implies simultaneous variation of both tectonic activity, such as earthquakes, and climatic properties; such as the global temperature represented by the model. The model therefore also holds promise for earthquake forecasting.

A theory is proposed to explain the alternation of earthquake activity between different areas over a period of time. This is tested in hindcast for the many twentieth century earthquakes of Magnitude 6 or greater on the Richter scale in China. Within the limitations of the accuracy of small scale topographic mapping and suspected insensitivity of epicentre location, the results are most encouraging.

Key Words: Universal gravitation constant, Earthquake, China

BACKGROUND

Natural disasters appear to plague mankind today more than at any time in the past, perhaps because there is now more of mankind to plague, perhaps because communications are more efficient, or possibly because disasters are increasing in frequency. Few natural hazards are more devastating than a large earthquake. In practical terms even an event of Magnitude 6 on the Richter scale of earthquake intensity is an awesome demonstration of tectonic activity; Magnitude 8 lays waste like a nuclear bomb. China has experienced more than 200 earthquakes of Magnitude 6 or more since 1900.

Many scientists have devoted themselves to attempts to unravel the causes of these events and to forecast their occurrence. Little wonder, considering such tragedies as the 1976 earthquake of Tangshan, which resulted in the death of about 200,000 people and destruction of property equivalent to the total amount of construction in that area since 1949. The massive scale of the problem justifies the consideration of a wide range of

research into forecasting methods, from the relatively conventional advances by Rikitake (1982) to the more premonitory approach by Tributsch (1982). Notable successes have been demonstrated for some but still most events occur unexpectedly.

During the last decade a new technique has been explored for forecasting the climate, another geophysical phenomenon. It was introduced in principle by Denness (1981) who described the concept of matching a simple mathematical equation to observed climate-related time series over many different time scales from a few years duration to a period of over 3 billion years—about $\frac{2}{3}$ the commonly accepted age of the solar system and hence the Earth. Many supporting examples were given by Denness (1984 a and b) of the close match of hindcasts from the equation with a broad range of measured data gleaned from the literature. Though many climatologists (e. g. Hays et al., 1976) have attempted to derive the components of climatic variation during particular timescales and illustrated their apparent relationship to various astronomical cycles, such as those explored by Milankovitch (1938), this represented the first recognition of orderly climatic variability across all measurable climatic time scales. The observed data, and consequently the variation represented by the equation which closely matches them, all relate to regional climate which exhibits at least an overall correlation with the global temperature; some are directly related to it.

It is a short step from this to a conceptual model for earthquake prediction. However, that step embraces a wealth of implications for our understanding of physical concepts.

First let us examine the formulation of the equation and its further substantiation by its comparison with measured time series during the historical period.

THE EQUATION

The equation is first presented in the empirical way in which it was derived. Its higher frequencies are then tested against several sets of climate-related data, they being the most commonly available evidence of past variability in the physical environment, before the link is forged with earthquake activity. This also lays the foundation for elevating this approach from its empirical roots to a sounder analytical basis.

The seabed contains the basic information which sparked off the climatic study. Ear-

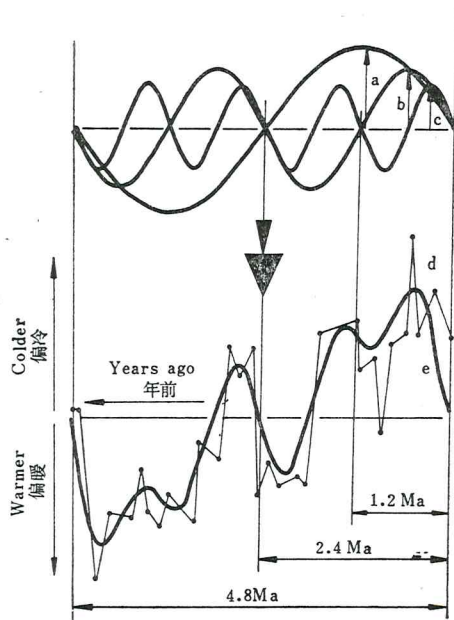


Fig. 1 Combination of sinusoidal components.

图1 正弦分量的组合

lier marine geotechnical studies led on to the recognition of systematic variation in oxygen isotope profiles deep into the seabed. These records describe the variation of past climate: the deeper into the seabed the older the climatic record; the higher the isotope index the colder the climate. The first record studied was of a sedimentary sequence some seven million years old representing almost continuous deposition off the Azores in the North Atlantic recorded by Shackleton and Cita (1979). A qualitative assessment illuminated a major cyclic trend of oxygen isotopes of sinusoidal form with a period of about 4.8 million years. Superimposed on this cycle was a further sinusoidal trend of smaller amplitude and period 2.4 million years to which was added another even smaller scale variation of period 1.2 million years as shown in Figure 1.

The Figure illustrates the sum of these sine components to simulate approximately the observed isotope record. The three sine components were the first to be discovered in a series which was eventually traced back through other climate records to over a billion years in period and down to only a few years or less with every successive component being of half the period and 0.84 times the amplitude of its more fundamental neighbour. The equation which represents this variation is consequently:

$$G(t) = \sum_{n=N(T)}^{\infty} A(T) a^n \sin b^{1-n} \pi \left(\frac{t}{T} \right) \quad (1)$$

Zero registered at time T_0 .

Where $G(t)$ is a time based climatic index

$A(T)$ is the amplitude of a reference periodicity T

$N(T)$ is the reference integer for periodicity T

a, b are absolute constants, here taken as 0.84 and 0.50 respectively

n is an integer, i. e. the reference number of a particular sine component

and t is time in years

TESTING THE EQUATION IN HISTORICAL TIME

Denness (1984a) described the matching of climatic hindcasts from the equation, after smoothing its graphic output, to measured climatic series over periods ranging back from the present to 3,000,000,000 years ago down to the shorter duration from the present to 1,800,000 years ago. Shorter period variations of the equation and their correlation with observed climatic time series were also explored by Denness (1984b) over timescales from zero to 1,000,000 years ago down to the historical period from the present day to 1,800 years ago. In total these two studies exposed the consistent variation of global temperature over most of the Earth's history with cumulative periodicities representing components ever halving from the most fundamental recognisable of 1.12×10^9 years, the shortest being 1,090 years.

Here additional measured time series are taken from the published literature to illu-

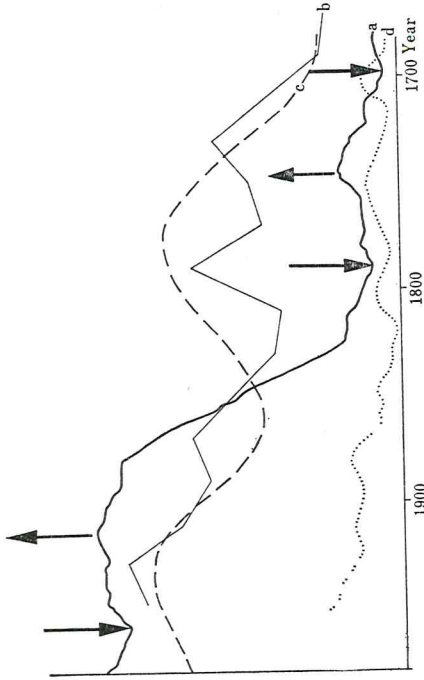


Fig. 3 Comparison of climatic indices and model on the timescale 0-300 years before 1980.
 图3 1980年前0-300年时间内气候指数与模式的对比
 a. Model; b. Tree ring widths at upper tree line in the White Mountains of California, U.S. A.; c. Temperature in China; d. Position of glacier terminus in Savoie Alps;

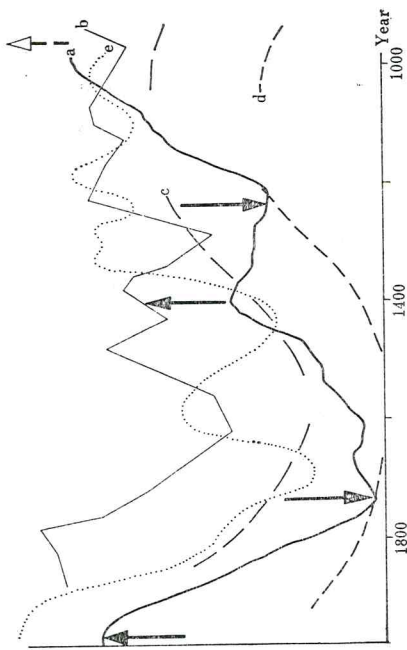


Fig. 2 Comparison of climatic indices and model on the timescale 0-1000 years before 1980.
 图2 1980年以前的1000年时间内模式和气候指数的对比
 a. Model; b. Deuterium proportion in bristlecone pines of California; c. Drift of winter severity index across Europe at 50°N; d. Drift of high summer wetness index across Europe at 50°N; e. Winter conditions in eastern Europe

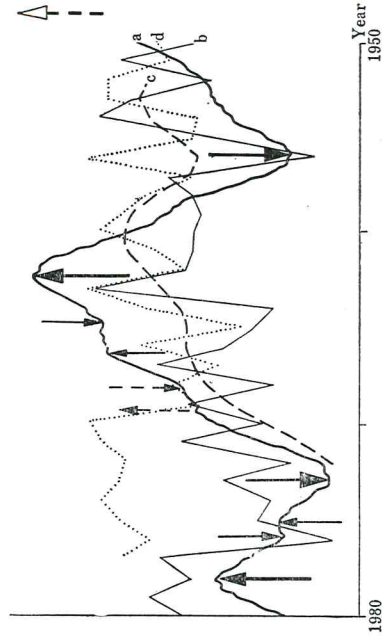


Fig. 5 Comparison of climatic indices and model on the timescale 0-30 years before 1980.
 图5 1980年以前0-30年时间内气候指数与模式的对比
 a. Model; b. Northern hemisphere autumn temperature; c. Annual temperature at Eureka, Canada; d. Winter snow at Lerwick, Shetlands

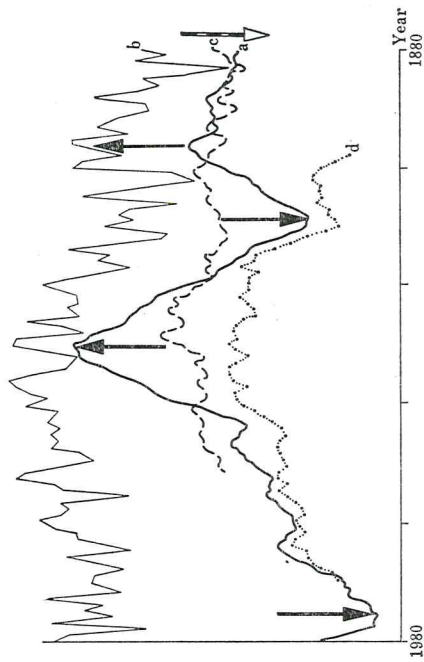


Fig. 4 Comparison of climatic indices and model on the timescale 0-100 years before 1980.
 图4 1980年以前0-100年时间内气候指数与模式的对比
 a. Model; b. Northern hemisphere summer temperature; c. Accumulation of snow at the South Pole; d. Date of capture of spawning Arctic-Norwegian cod at Lofoten

strate further their matching with hindcasts from the equation and to substantiate its application down to periods of climatic variation of only a few years, consistent with the timescale over which earthquake activity is then examined. Previously Denness (1984c and d, 1985 and 1987) and Burns and Denness (1985) covered these timescales in the contexts of forecasting water resources, global and regional economy, the Greenhouse Effect, sea level rise and agricultural changes. The longest climate-related records used here are shown in Figure 2 superimposed on the plot of $G(t)$, smoothed by the moving average technique described by Denness (1984a and b). Extending over 1,000 years before the present it is seen that all four records exhibit the same major trend as the graphic output from the equation (1) from a warm period in the Middle Ages, through a cold period (the Little Ice Age) which was most severe in the eighteenth century, to return to a warmer climate this century; this emphasizes a periodic variation of about 1,090 years. These records are the proportion of deuterium in bristlecone pines of California described by Lamb (1977) from data provided by I. Friedman; the drift of both the winter severity index and the high summer wetness index across Europe at 50°N also described by Lamb (1977); and winter conditions in eastern Europe extracted from manuscript records by Lamb (1969). In addition, the trend of the proportion of deuterium in bristlecone pines of California can be correlated with an additional maximum and minimum of the graphic output from the equation (arrowed) demonstrating the next component in the series of period 545 years.

Figure 3 shows the general trend from equation (1), the climate model, to be an approximate mean representation of the trends of the three measured time series, tree ring widths at the upper tree line in the White Mountains of California reported by Lamb (1977) using data provided by V. C. LaMarche, temperature variation in China from Chu (1973) and the position of a glacier terminal in the Savoie Alps from Ahlmann (1953). The glacier terminal position exhibits a trough between two peaks at about 272 years apart, the next component in the series. The general trend of both the other two measured climatic time series also points towards correlation with the closer maxima and minima reflecting a climatic variability component of the next anticipated period of about 136 years.

The correlation is continued into the so-called instrumental period in Figure 4. Here is emphasized the matching of the expected approximate 68-year climatic cycle of the model with that of the northern hemisphere summer temperature from Jones and Wigley (1980a) and the date of capture of spawning Arcto-Norwegian cod at Lofoten reported by Cushing and Dixon (1976). To a lesser degree this observation is also supported by the measurements of the accumulation of snow noted by Fletcher (1969).

Figure 5 represents a period which is contained within the lifetime of most adults. Finding no evidence of the next anticipated component in the sine series a 34 year per-

iod-it nevertheless illustrates a strong 17-year periodicity in both the model and the variation of northern hemisphere autumn temperature reported by Jones and Wigley(1980b). This is also reflected to a lesser degree in the shorter record of annual temperature at Eureka in Canada from Jones (1976). Both the northern hemisphere autumn temperature record and the winter snow observations at Lerwick in the Shetlands, described by Morth (1978), draw attention to the correlation of their shorter periods of variation with those of the model at about 4.2 and 2.1 years while the Canadian record fills the gap in the series with a correlated component of period 8.5 years.

This short set of examples consequently illustrates the observation from measured climatic time series of 9 of the 10 components of the anticipated sine series from the climatic model over the historical period since the Middle Ages. These components are to be added to the longer period cycles noted from the earlier publications by Denness (1984a and b) giving a combined series of 26 of the expected 30 components in the orderly sine series periodicities starting at about 1.25×10^9 year period and ending here at 2.1 years. Either directly or indirectly the observed time series are all related to global temperature. Consequently the model represented by the curve from the equation, and hence equation (1) itself, also describes global temperature.

AN EXPLANATION OF SYSTEMATIC GLOBAL TEMPERATURE VARIATION

Building on the pioneering work of Croll (1875), Milankovitch (1938) established the commonly held theory of the impact of astronomical factors on the Earth's climate. This popular theory explains correlations between the warming and cooling of the Earth and variations in its orbital and other astronomical properties. Let us now introduce another element to this approach. Instead of just accepting orbital variations at face value let us consider instead the relationship between the semi-major axis of revolution, a , and Newton's Gravitational Constant, G , described by Lyttleton (1982) while questioning the constancy of G as:

$$\frac{\dot{a}}{a} = -\frac{\dot{G}}{G} \quad (2)$$

In turn, from the inverse square law of radiation we have:

$$T = \frac{K}{a^2} \quad (3)$$

where T is the temperature at the surface of a cold body (the Earth) at a distance, a , from a hot body (the Sun) and K is a constant.

From (3),
$$\dot{T} = -\frac{2K}{a^3} \dot{a} \quad (4)$$

∴ by dividing equation (4) by equation (3),

$$\frac{\dot{T}}{T} = -\frac{2\dot{a}}{a} \quad (5)$$

Rearranging (5):

$$\frac{\dot{a}}{a} = -\frac{1}{2} \frac{\dot{T}}{T} \quad (6)$$

Substituting (6) in (2):

$$\frac{\dot{G}}{G} = \frac{1}{2} \frac{\dot{T}}{T}$$

i. e. the rate of change of G with respect to its absolute value is a half that of T with respect to its absolute value. Therefore, a change in G would be reflected by a simultaneous change in T . Consequently the many observations of variation in T throughout historical and geological time could have been brought about by simultaneous variations in G , represented by an expression of essentially the same form as equation (1), a concept previously introduced by Denness (1984e).

THE LINK WITH EARTHQUAKES

Having opened up the possibility that the foregoing observations of an orderly variation of global temperature since the early part of the Earth's history could imply an equally orderly variation of G , it is appropriate to consider the implications of this in other physical fields. The observation by, for instance, Lyttleton (1982) that a change in gravity would be accompanied by a change in the rate of rotation of the Earth is of potential relevance to earthquake forecasting. Observations which support this notion of rotational transience but appear to contradict the predicted direction are present in the records of varying length of day over the Phanerozoic timescale reported by Panella (1972). The observations are, in fact, largely directly consistent with the trend of temperature and G portrayed by the graphical output from equation (1) given by Denness (1984a). The consequences of a change in the rate of rotation would be a change in the centrifugal force exerted at any point on and within the revolving sphere of the Earth.

The change in centrifugal force would vary for a given mass subject to a given change in rate of rotation according to its distance from the axis of rotation as $F = mr\omega^2$, where F is the centrifugal force, m is the mass, r is the distance from the rotational axis and ω is the angular velocity.

The circumferential component of this force towards the equator, F_e , is seen from Figure 6 to be $F \cos \theta$.

i. e.

$$F_e = mr\omega^2 \cos \theta$$

but

$$r = R \sin \theta$$

∴

$$F_e = mR\omega^2 \sin \theta \cos \theta = \frac{mR\omega^2}{2} \sin 2\theta$$

$$\therefore \frac{\Delta F_c}{\Delta \theta} = mR\omega^2 \cos 2\theta$$

At a maximum or minimum $\frac{\Delta F_c}{\Delta \theta} = 0$

i.e. $mR\omega^2 \cos 2\theta = 0$

i.e. $\theta = \pi/4$

But $\frac{\Delta^2 F_c}{\Delta \theta^2} = -2mR\omega^2 \sin 2\theta$

\therefore at $\theta = \pi/4$, $\frac{\Delta^2 F_c}{\Delta \theta^2} = -2mR\omega^2$

i.e. at $\theta = \pi/4$ $\frac{\Delta^2 F_c}{\Delta \theta^2}$ is negative $\therefore \frac{\Delta F_c}{\Delta \theta}$ is a maximum

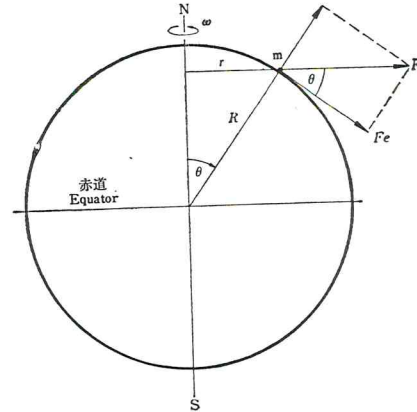


Fig. 6 Resolution of centrifugal force.

图6 离心力的分解

That is to say that at $\theta = \pi/4$ (45° latitude North or South) the change in the tangential force between two given masses at the surface of the Earth caused by a change in G would be greater than elsewhere. One might, therefore, anticipate that seismic activity induced by a change in circumferential forces between plates might be greatest at points between a plate at that latitude and another elsewhere, all other geological factors being excluded. Is it coincidence then that many of the regions of the world most noted for earthquakes are within a small angle of arc from that latitude, e. g. Northern China, Korea, Japan, California, Chile, New Zealand, Italy, Greece and Turkey? Many of the other seismically active regions outside this belt would also experience circumferential movement induced by the influence of maximum G variation transferred through intact plates which themselves only partially occupy that belt (e. g. those around the Pacific plate). However, the seismic activity around the oceanic plates is thought to be only partially due to this mechanism as those plates are continually moving towards and subducting beneath the continental plates irrespective of the influence of G .

Pursuing this conceptual model a little further may hold promise of allowing the combination of these secular and geometric elements. Let us consider the example of the Chinese mainland. In very broad terms the western and largest part of this region lies between the Siberian platform and the Indian platform and corresponds roughly to the boundary of the Himalayan mountains and outlying ranges. Figure 7 expresses this situation crudely in diagrammatic terms and explores the expected reactions of the folded sedimentary units between the two platform to a change in G according to the foregoing argument. Parts (a) and (b) illustrate the compression zones encountered in compressing or extending folded strata from basic strength-of-materials theory. At the bottom of the figure is an equally simple illustration of the physical geography principle that erosion leads to the formation of hill and valley structures as shown. Combining these two themes leads to the anticipation of compression-generated earthquakes in present-day val-

leys at times of high G and in present-day hill ranges at times of low G , these being respectively the location of the most vulnerable parts of a given highly stressed stratigraphical horizon in the two conditions of G .

EARTHQUAKE PREDICTION

Here then is a testable theory. The earlier part of this article sought to extend previous work on geological and historical climate modelling into the timescale of the present century. This was followed by the demonstration of a possible mechanism to relate climate variation to G , the so-called Universal Gravitational Constant. In Figure 8 there is a hindcast of the variation of G since 1900 using this approach.

The diagram can be divided into time zones of low and high G as shown. According to the above theory it would consequently be expected that periods of major seismic activity in China since 1900 (for example, as these are well documented by Anon, 1979) would locate themselves in locally lowland areas, i. e. overall concave upwards, during the periods 1900-1902, 1924-1939 and 1958-1972, whereas they would be in locally upland areas, i. e. overall convex upwards, during the intervening periods and from 1972-1979, the date of the latest information on the source map.

Figure 9 describes the location of all major earthquakes (of Magnitude 6.0 to 8.5 on the Richter scale) which are recorded by the geophysical map of Anon (1979) as having occurred in China during the period 1900-1979. The geophysical map bears witness to such quakes, all of which are dated precisely. Figure 9 superimposes these locations on a generalized topography

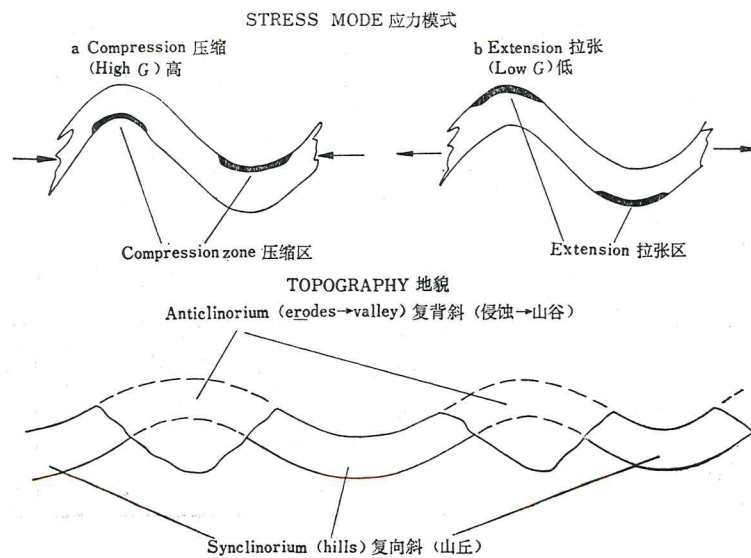


Fig. 7 Strata response to lateral stress.

图7 地层对侧向应力的反应

determined from a 1:20,000,000 scale map by Fullard and Darby (1976); although working on this small scale introduces scope for subjective error it can be suggested that it is nevertheless adequate for a conceptual introduction. The earthquakes are differentiated into the above two groups of chronological zones.

It is submitted that the association of quakes during each of the two groups of time-zones with lowlands and uplands respectively is striking. Even allowing for considerable error in the definition of the local upland/lowland boundaries and the inherent imprecision in locating the epicentres of quakes which may often be extensive so that several of the more dubious locations (denoted by underlining) might be in neighbouring areas and hence reverse topography, the association would seem too pronounced to be the

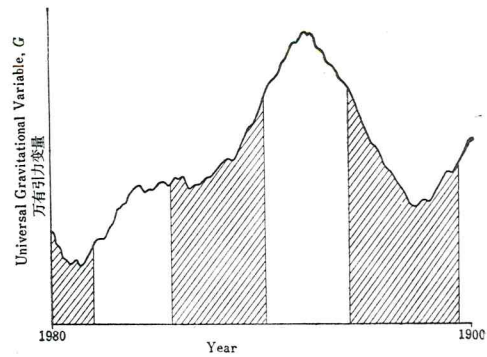


Fig. 8 Twentieth century variation of G .

图8 二十世纪 G 的变化

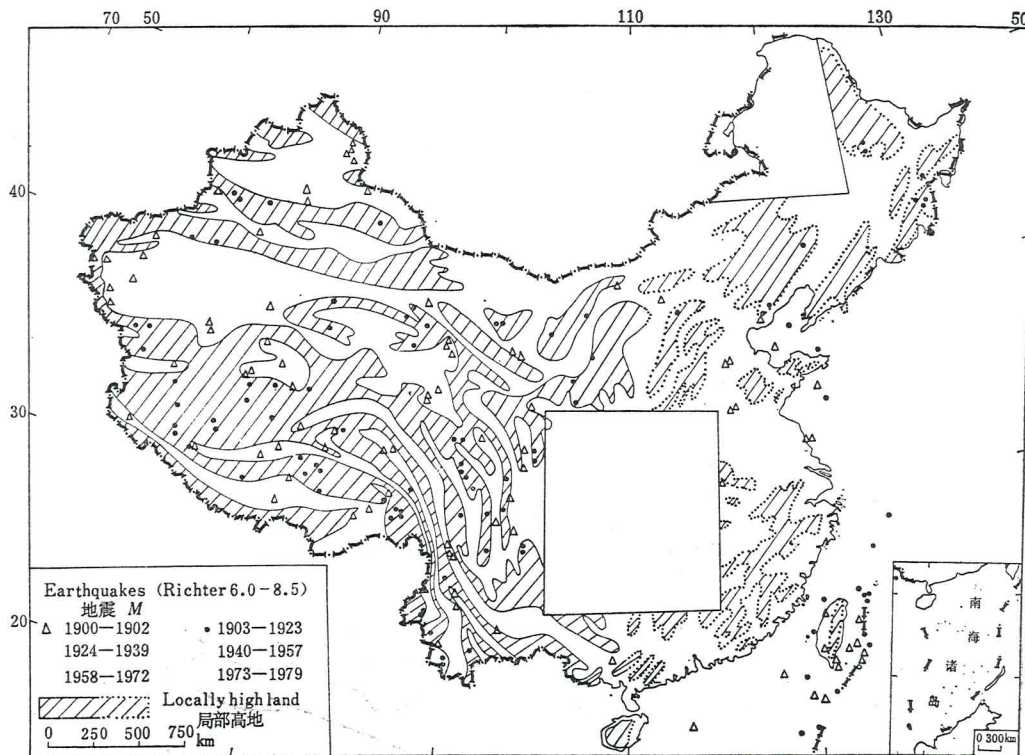


Fig. 9 Twentieth century high-energy earthquakes in China.

图9 二十世纪中国的高能量地震

result of mere coincidence. This is all the more so in the light of the foregoing theory which volunteers an explanation of the association.

The case thus temporarily rests. But what of the future? It is as easy to extend the mathematical model encapsulated in the thick black line of Figure 8 into a forecasting mode for the future as it is to use it as shown here to match the past. Equally it would be possible to examine likely movements resulting from changes in centrifugal forces between plates induced by a varying G in other regions of the world. Combining these two factors could lead to the possibility of preparing both a short and long term forecasting model for global earthquake activity. In addition, by inference, it might be expected that further resolution on smaller geographical and energy scales might enable the forecasting of smaller quakes than those of Magnitude 6 or more described here and thereby increase the sensitivity of regional forecasting.

In view of the promising start of this approach in China it would seem sensible to pursue the study both in more detail in the same area and also at the same degree of interpretative sensitivity in neighbouring areas. Among these would be Hong Kong, where it is reasonable to suppose that even a moderate earthquake would have a significant impact on slope stability and construction, and the Chinese offshore oil provinces in which the siting and design of production facilities could benefit considerably by knowledge of the likelihood of major seismic activity during their relatively short lifetimes.

CONCLUSION

In conclusion it should be recounted that this paper sets out to fulfil four main ambitions:

to consolidate a climate forecasting model hitherto developed over geological and historical timescales by providing a vehicle for hindcast testing over recent historical and modern timescales;

to illustrate the possibility that such a model may equally well describe a secular variation of the Universal Gravitational "Constant" G ;

to apply this concept to the matching of the earthquake record for China during this century to that anticipated from the model;

and to open the possibility that this approach may be used to allow the forecasting of earthquakes on both a regional and temporal basis to complement parallel work on climate forecasting.

There may appear to be ample room for incredulity but, nevertheless, the theory is supported by a wealth of sound measured data which compares favourably with a predetermined mathematical model and is considered worthy of presentation at this early stage in view of the enormous saving of life and property which will result from its further substantiation.

ACKNOWLEDGEMENTS

The author wishes to acknowledge a helpful discussion with members of the Global Seismology Unit of the British Geological Survey, Edinburgh, U.K. From this it was recognised that more detailed mapping of morphology and qualification of epicentre locations would be required to extend this study beyond the conceptual level in which it is presented here.

(Received in Aug. 1987)

REFERENCES

- [1] Ahlmann, H. W., 1953, Glacier variations and climatic fluctuations. Bowman Memorial Lecture, New York (American Geographical Society), in Lamb, H. H. (1977 op. cit.).
- [2] Anon, 1979, The geophysical map of China. Chinese Geological Institution (Team No. 562). Beijing.
- [3] Burns, R. and B. Denness, (1985), Climate and social dynamics: the Tripolitanian example 300BC-AD300, Town and Country in Roman Tripolitania, British Archaeological Reports, International Series 274, Oxford, pp. 201-225.
- [4] Chu Ko-Chen 1973: A preliminary study of the climatic fluctuations during the last 5,000 years in China, *Scientifica Sinica*, 16(2), Beijing, pp. 226-256.
- [5] Croll, J., 1875, Climate and time, Appleton and Co., New York.
- [6] Cushing, D. H. and R. R., Dixon, 1976, The biological response in the sea to climatic changes, *Adv. mar. Biol.*, 14, pp. 1-122.
- [7] Denness, B., 1981, How to build an ocean, *Proc. Conf. Oceans 81*, IEEE, Boston, pp. 341-344.
- [8] Denness, B., 1984a, An analytical climate model: application to the southern hemisphere Quaternary period, *Proc. Int. Symp. Late Cainozoic Palaeoclimates of the southern hemisphere* (ed. J. C. Vogel), Balke-ma, Rotterdam, pp. 35-42.
- [9] Denness, B., 1984b, The coincidence of a general climate model and historical climatic observations in East Asia, *Proc. Conf., The Evolution of the East Asian Environment* (ed. R. O. Whyte), 1, Hong Kong University Press, pp. 199-219.
- [10] Denness, B., 1984c, Water resource forecasting, *Proc. 4th IAHR Conf. on Water Resources Development and Management, II*, Chiang Mai, Thailand, pp. 1177-1194.
- [11] Denness, B., 1984d, The climate-energy-economy link, *Energy Exploration and Exploitation* 1(3), Graham and Trotman Ltd., London, pp. 61-69.
- [12] Denness, B., 1984e, The Greenhouse Affair. *Marine Pollution Bulletin* 15(10), Pergamon, Oxford, pp. 355-362.
- [13] Denness, B., 1985, Greenhouse dilemma. *Nature* 318, p596.
- [14] Denness, B., 1987, Sea level modelling: the past and the future, *Prog. Oceanog.*, 18, Pergamon, Oxford, pp. 41-59.
- [15] Fletcher, J. O., 1969, Ice extent on the Southern Ocean and its relation to world climate. Memorandum RM-5793-NSF. Santa Monica, California (Rand Corporation).
- [16] Fullard, H. and H. C. Darby, 1976: *The University Atlas*. Philip., London, p111.
- [17] Hayes, J. D., J. Imbrie and Variations in the Earth's orbit: pacemaker N. J. Shackleton 1976, of the Ice Ages, *Science*, 194, pp. 1121-1132.
- [18] Jonest P. D., 1976, Annual mean surface temperatures, *Eureka, Climate Monitor*, 5(1), CRU, University of East Anglia, Norwich, p.24.
- [19] Jones, P. D. and T. M. L. Wigley, 1980a, Northern hemisphere summer temperature, 1881-1980. *Climate Monitor*, 9(3), CRU, University of East Anglia, Norwich, p. 87.
- [20] Jones, P. D. and T. M. L. Wigley, 1980 b, Northern hemisphere autumn temperatures, 1881-1980, *Climate Monitor*, 9(4), CRU, University of East Anglia, Norwich, p. 110.
- [21] Lamb, H. H., 1969, Climatic fluctuations, in world survey of climatology, 2, *General climatology* (ed. H. Flohn), Elsevier, New York, pp. 173-249.
- [22] Lamb, H. H., 1977, *Climate: present, past and future*, 2: Climatic history and the future. Methuen, London, 835p.

万有引力常数的变化与 中国地震的时-空分布

B. 丹内斯

(英国应用科学局)

摘 要

地震是破坏性很大的自然灾害,世界上没有一个地方比中国和东亚沿海地区经历过更多的地震。同样的,干旱、洪水以及其它气候灾害也是世界上屡见不鲜的事件。本文提出了将这两种地球物理现象联系起来的理论。

早在80年代初期,便已提出气候变化的决定性的分析模式。该模式与古气候时间序列相符合,并可用于预报,它成功地经受过几年的检验。早先对该模式在地质时标上的核实,在这里我们将之延伸到近代历史。并且根据万有引力常数(G)随时间变化的可能性提出了关于气候变化原因的解釋。 G 的变化意味着构造活动性(如地震)与气候特性(如由模式所表示的全球温度变化)的同步变化。因此,该模式也为地震预报提供了希望。

作者提出了解释在某一时间段内不同地区地震活动性的交替的理论。该理论通过对中国廿世纪发生的里克特震级大于或等于6的许多地震的检验。在小比例尺地形制图精度以及在震中定位的低灵敏度范围内,所获结果是令人鼓舞的。

关键词: 万有引力常数 中国 地震

(上接64页)

- [23] Lyttleton, R. A., 1982, *The Earth and its mountains*, Wiley and Sons, Chichester, pp. 177-193.
- [24] Milankovitch, M., 1938, *Astronomische Mittel zur Erforschung der erdgeschichtlichen Klimate*, in *Hanbuch der Geophysik*, 9 (ed. G. Gutenberg), Berlin, pp. 593-698.
- [25] Morth, H. T., 1978, Severe snow drifts over Scotland and southwest Britain, *Climate Monitor*, 7(1), CRU, University of East Anglia, Norwich, pp. 23-28.
- [26] Pannella, G., 1972, Palaeontological evidence on the Earth's rotational history since Early Precambrian. *Astrophys. Space Sci.* 16, pp. 212-237.
- [27] Rikitake, T., 1982: *Earthquake forecasting and warning*, Centre for Academic Publications Japan, Tokyo, 402p.
- [28] Shackleton, N. J. and M. B. Cita, 1979, Oxygen and carbon isotope stratigraphy of benthic foraminifera at Site 397: detailed history of climate change during the late Neogene, Initial Report of Deep Sea Drilling Project 47, US Government Printing Office, Washington DC, pp. 433-445.
- [28] Tributsch, H., 1982, *When the snakes awake: animals and earthquake prediction*. MIT Press, Mass., USA, 248p.

河北怀来黄土窑古地震剖面

方仲景 程绍平 王景钵 李志义 袁著忠

(国家地震局地质研究所)

最近,我们在执行国家地震局下达的延庆—怀来盆地活断层填图任务的踏勘中,于怀来县城西北8公里的黄土窑村发现一古地震剖面(图1)。古地震表现为第四纪断层的形式。在剥露剖面的长11米范围内共有十余条断层,它们的走向为北45°西,倾向南西,倾角60°到近于直立,主断层宽度达2—4米(图2)。

1. 地质构造和地貌背景

该剖面位于黄土窑村西南。在构造上处于怀来盆地北部边缘北60°东和北西西向两断裂的交汇部位,前者规模较大,延伸较远;后者规模较小。在第四纪期间,这两组方向的断层均表现出明显的活动性。北60°东方向的断层使得Q₃黄土与侵入到震旦亚界雾迷山组含燧石条带白云岩中的基性岩脉呈断层接触,形成约数十米宽的灰绿色断层泥和破碎带,部分Q₃黄土块体被卷入断层泥中。从沿北60°东断层走向开挖断层泥的巷道观察表明,灰绿色断层泥带在与北西西向断层交汇部位突然中断,推测它已被北西西向断层所错断。

古地震剖面暴露于以这两组断层为界的山前地带残余古冲积扇台地边缘。一条近南北向的冲沟从北部山中流出切割了该古冲积扇,后来的

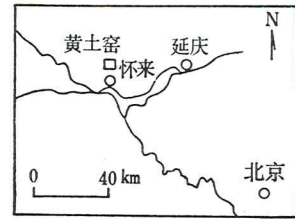


图1 怀来黄土窑古地震剖面位置

Fig.1 Location of the paleoseismological section, Huangtuyao.

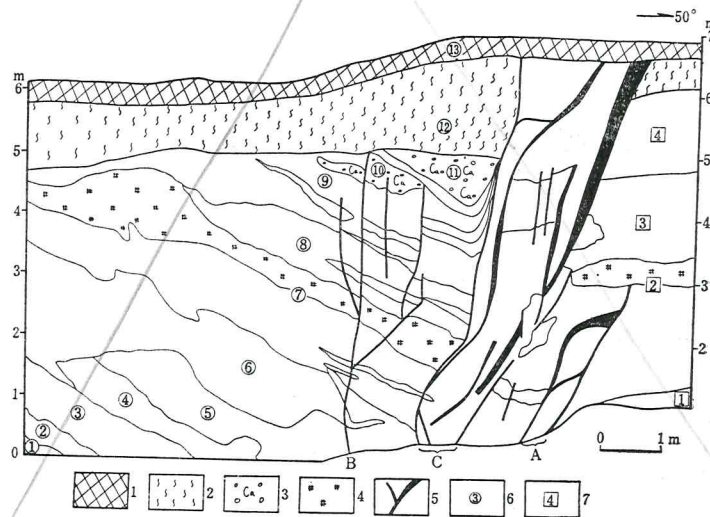


图2 怀来黄土窑村西南剥露的古地震剖面

Fig.2 Log of the section stripped at Huangtuyao, Huailai, showing Paleoseismicities.

1. 现代古壤; 2. 具有钙质丝状物和极薄钙膜的亚粘土沉积物; 3. 砾石表面有薄的钙膜、砾石间充填以钙物质的钙土壤; 4. 砾石表面有较厚的钙膜、砾石间有大量的钙质充填, 和具有较厚碳酸钙淀积层的钙土壤; 5. 断层; 6. 断层上盘的岩性层序号; 7. 断层下盘的岩性层序号